Hindawi Publishing Corporation
Journal of Nanomaterials
Volume 2014, Article ID 725356, 14 pages
http://dx.doi.org/10.1155/2014/725356

Research Article

Equilibrium and Nonequilibrium Nanoscale Ordering of Polystyrene-*b*-poly(*N*,*N*′-diethylaminoethyl methacrylate), a Block Copolymer Carrying Tertiary Amine Functional Groups

Pedro Navarro-Vega,[1] Arturo Zizumbo-López,[1] Angel Licea-Claverie,[1] Alejandro Vega-Rios,[2] and Francisco Paraguay-Delgado[2]

[1] *Instituto Tecnológico de Tijuana, Centro de Graduados e Investigación en Química, Apartado Postal 1166, 22000 Tijuana, BC, Mexico*
[2] *Centro de Investigación en Materiales Avanzados (CIMAV), Complejo Industrial Chihuahua, 31109 Chihuahua, CHIH, Mexico*

Correspondence should be addressed to Angel Licea-Claverie; aliceac@tectijuana.mx

Received 11 July 2014; Revised 15 October 2014; Accepted 29 October 2014; Published 27 November 2014

Academic Editor: Wanqin Jin

Poly(styrene)-*b*-poly(*N*,*N*′-diethylaminoethyl methacrylate) (PS-*b*-PDEAEM) block copolymer was synthesized by RAFT free-radical polymerization using a trithiocarbonate type of chain transfer agent (CTA). Several block copolymer compositions were achieved maintaining low polydispersities by using PS as macro-CTA in the first step. Thin films of $PS_{60\%}$-*b*-$PDEAEM_{40\%}$ were deposited over mica substrate, and its equilibrium and nonequilibrium nanostructures were studied. Lamellar (equilibrium), bicontinuous (nonequilibrium) and detached nanoflakes (nonequilibrium), were obtained by using different annealing methods. Mixing nanocomposites of gold nanoparticles/PDEAEM in the block copolymer resulted in the formation of toroidal nanostructures confining gold nanoparticles to the core of those nanostructures. The same toroidal nanostructure was achieved by different annealing methods, including irradiation with UV light for 15 min. Electron micrographs show clearly this different type of arrays.

1. Introduction

Block copolymers (BCPs) of immiscible blocks are comprised of two chemically different chains covalently linked at one end. BCPs self-assemble into various morphologies in thin films depending on the following parameters: volume fractions of the blocks (f), molecular weight of BCP, interaction parameter between the blocks (χ), interfacial interactions with substrate, film thickness relative to natural block copolymer periodicity, and type of solvent used and its evaporation rate [1–9]. According to the phase diagram by Matsen and Bates, at thermodynamic equilibrium, self-assembly into lamellar, cylindrical, spherical, or gyroid nanostructures can be achieved, depending on f and molecular weight times interaction parameter (χ) of the BCPs [3]. In principle, the same four nanostructures can be achieved for all BCPs of immiscible blocks. However, one key factor in the practical use of block copolymers is the control over the orientation and lateral ordering of the morphologies in thin films [10]. Generally, the order in thin films of block copolymers can be improved by means of thermal annealing [8, 11–16] and solvent annealing [2, 7, 17, 18], among other methods. For thermal annealing, there usually exists only a small temperature window between the glass transition temperature (T_g) and the degradation temperature (T_D) of the involved blocks which are usually susceptible to thermal degradation [19]. Solvent annealing provides an attractive alternative to thermal annealing, since sufficient mobility of the block chains is easily induced at room temperature without the danger of degradation of the block copolymer, although some low vapor pressure solvents would need some thermal aid to induce phase separation [20–22]. The solvent annealing approach has been used more and more widely in recent years [23]. However, the details of solvent annealing remain rather

unclear since the relevant experimental parameters governing the resultant block copolymer nanoscale morphologies (nature of the solvent, the relative solvent vapor pressure, the annealing time, etc.) are usually complex and difficult to control [24]. Among these factors, the nature of the solvent and the relative solvent vapor pressure are crucial [25]. The nature of the solvent influences the degree of the swelling of each block and accordingly has severe effects on the resulting block copolymer morphologies [7]. It has been shown that the same block copolymer thin films annealed under different selective solvents and nonselective solvents result in different morphologies and orientations [7, 26]. On the other hand, once a solvent is selected, the solvent vapor pressure is the key factor to control the resultant morphologies [27, 28]. It has been reported that regular phase separated films can only be achieved when the copolymer Hildebrand solubility parameter is very similar to the value of the solvent used for annealing [26]. A lot of practical know-how has been reported in order to control the solvent vapor pressures, such as the use of the flow of N_2, to vary the amount of solvent in reservoir, to close the lid of dish more or less tightly, and to change the ratio between the surface area of the solvent and the empty volume of the annealing chamber [17, 23, 29, 30]. In thin films, the destabilization of films is another important technical issue that should be considered for pattern formation [31]. Under certain conditions, the local fluctuation of film thickness is developed, and the film is retracted from the substrate to create fragmentation of continuous films into isolated droplets.

Due to the intrinsic nature of polymer chains, the obtained nanostructures (in solution, bulk, or thin films) may be kinetically trapped nonequilibrium systems, since the constituent polymer chains may not be able to relax towards their equilibrium conformation [32].

When polymers carrying functional groups in one of the blocks are investigated towards nanoscale ordering in thin films, a new factor can be included to increase the richness of self-assembled nanostructures that are achievable: small molecules capable of forming complexes with the functional groups of the one block. A well-studied example of this approach is the use of poly(styrene)-*b*-poly(4-vinylpyridine) (PS-*b*-P4VP) in combination with 2-(4′-hydroxybenzeneazo)benzoic acid (HABA) by Tokarev et al. [33], Sidorenko et al. [34], Böhme et al. [35], and Nandan et al. [36].

In our research group, we are interested in the study of equilibrium and nonequilibrium self-assembled nanostructures formed by poly(styrene)-*b*-poly(*N,N*′-diethylaminoethyl methacrylate) (PS-*b*-PDEAEM). PDEAEM is a polymer carrying tertiary amine groups capable of acting as proton acceptors and lone pair donors (Brönsted and Lewis bases) and also capable of coordinating with metals having d and f orbitals with deficit on electrons. To the best of our knowledge, the only report on the study of self-assembled thin films of this BCP was recently published [37]. PS-*b*-PDEAEM was studied together with the parent BCP, poly(styrene)-*b*-poly(*N,N*′-dimethylaminoethyl methacrylate) (PS-*b*-PDMAEM) in blends with polystyrene finding that they formed micellar and donut-like structures over thin films independent of the parameters changed. The main difference between PDEAEM and PDMAEM blocks is their hydrophobicity and acidity constant (pK_a): while PDMAEM is soluble in water at neutral pH and has a pK_a of 8.1 [38], PDEAEM is only soluble in water at pH values close to 6 and lower, while it has a pK_a of 6.9 [39].

In the current report, not only the equilibrium and nonequilibrium self-assembly process of PS-*b*-PDEAEM was investigated in detail, but also the interactions of gold nanoparticles (AuNPs) and their role in self-assembly process of the title BCP was assessed.

2. Experimental Section

2.1. Materials. All reagents were purchased from Sigma-Aldrich (Mexico) and were used as received with the exception of those described below. Styrene and *N,N*′-diethylaminoethyl methacrylate (DEAEM) were distilled under reduced pressure to the highest purity possible. 4,4′-Azobis(4-cyanovaleric acid) (ACVA, Fluka) was recrystallized from methanol. 4-Cyano-4-(dodecylsulfanylthiocarbonyl)sulfanyl pentanoic acid (CTA) was synthesized following a procedure reported in the literature [40] and was obtained with 72% yield.

2.2. Synthesis of Macro-CTAs by RAFT Polymerization. All polymerizations were performed in ampoules. In all cases, 4-cyano-4-(dodecylsulfanylthiocarbonyl)sulfanyl pentanoic acid and 4,4′-Azobis(4-cyanopentanoic acid) were used as CTA and as initiator (ACVA), respectively. The appropriate amounts of monomers, CTA, and ACVA were dissolved in *p*-dioxane (30 mL) under stirring at room temperature. Solutions were degassed by three freeze-pump-thaw cycles. After degassing, the ampoules were flame-sealed under vacuum and heated in an oil bath at 90°C. The polymerizations were terminated by rapid cooling and freezing. The homopolymers obtained, also named macro-CTAs since they include the CTA moiety, were purified by repeated precipitations using methanol for polystyrene and petroleum ether for poly(DEAEM). Products were dried in vacuum for 48 h. An example of the synthesis of polystyrene is described in detail: styrene (12.02 g, 0.115 mol), 4,4′-Azobis(4-cyanopentanoic acid) (ACVA) (0.0485 g, 0.1203 mmol), and 4-cyano-4-(dodecylsulfanylthiocarbonyl)sulfanyl pentanoic acid (CTA) (0.0037 g, 0.0132 mmol) were dissolved in *p*-dioxane (30 mL) and poured in a glass ampoule (50 mL) containing a magnetic stir bar. Oxygen was removed using 2 freeze-thaw evacuation cycles, and the ampoule was sealed with flame under vacuum. The ampoule containing polymerization solution was submerged in an oil bath with magnetic stirring at 90°C. The polymerization was stopped by rapid cooling at a given time. The polymerization yield was obtained gravimetrically by adding a fivefold excess of cold methanol. The polymer product was purified by dissolution in the minimum amount of acetone followed by adding a fivefold excess of cold methanol and filtering. This procedure was repeated three times to remove residual monomer followed by drying under vacuum to constant weight.

2.3. Synthesis of Block Copolymers. The macro-CTAs obtained in the first step were characterized and used for the synthesis of diblock copolymers. The calculated amount of macro-CTA was dissolved in *p*-dioxane (15 mL) before adding different amounts of the second monomer and the initiator. The copolymerization procedure was the same as the synthesis of macro-CTAs by RAFT polymerization. For the purification of the block copolymers, a combination of solvent and nonsolvent for each copolymer was settled down according to their composition using petroleum ether/tetrahydrofuran(THF)/methanol. As an example, the detailed synthesis of a polystyrene-*b*-poly(DEAEM) block copolymer starting with a macro-CTA of polystyrene is described: polystyrene (1.0 g, 0.02443 mmol) M_n = 40,940 g/mol, ACVA (2 mg, 0.00714 mmol), and (3.9 g, 0.02105 mmol) of DEAEM were dissolved in *p*-dioxane (15 mL) containing a magnetic stir bar. Oxygen was removed using 3 freeze-thaw evacuation cycles, and the ampoule was sealed with flame under vacuum. The ampoule containing copolymerization solution was submerged in an oil bath with magnetic stirring at 90°C. The polymerization was stopped by rapid cooling at a given time.

The block copolymer was precipitated by adding a fivefold excess of cold methanol, decanting excess liquid, and dissolving the copolymer in the minimum amount of THF, precipitating again using cold petroleum ether and decanting again. This procedure was repeated three times to remove residual monomer and possible homopolymers formed. Finally, the product was dried under vacuum to constant weight. The copolymerization yield was obtained gravimetrically by this process of solution-precipitation of the copolymer.

2.4. Characterization of Block Copolymers

2.4.1. Nuclear Magnetic Resonance Spectroscopy (NMR). ^{1}H-NMR measurements were carried out on a Varian mercury (200 MHz) NMR instrument using chloroform-d as solvent and tetramethylsilane as reference. The main signals of NMR spectra for one example of each macro-CTA are described below. The multiplicity of signal is abbreviated as follows: *s* = singlet, *d* = doublet, *t* = triplet, and br = prefix for broad signal.

Macro-CTA of PS: M_n = 23,600 g/mol, PDI = 1.09. ^{1}H-NMR ($CDCl_3$, 200 MHz) δ 7.1 (3H, m, (Arom. 3CH)), 6.6 (2H, m, (Arom. 2CH)), 1.8 (1H, m, CH), and 1.4 (2H, m, CH_2).

Macro-CTA of PDEAEM: M_n = 22,500 g/mol, PDI = 1.17. ^{1}H-NMR ($CDCl_3$, 200 MHz) δ 4.1 (2H, m, O–CH_2), 2.6 (6H, m, N–$(CH_2)_3$), 1.8 (2H, m, CH_2), 1.1 (6H, m, $(CH_3)_2$), and 0.8 (3H, m, CH_3).

2.4.2. Gel Permeation Chromatography (GPC). The number-average molecular weight (M_n) and polydispersity of the molecular weight distribution (M_w/M_n) of the polymers were determined with a GPC Varian 9002 chromatograph equipped with two mixed-bead columns in series (Phenogel 5 linear and Phenogel 10 linear) and two detectors: refractive index (Varian RI-4) and triangle light scattering (MINI-DAWN, Wyatt Technology).

The measurements were performed in THF at 35°C at a flow rate of 0.7 mL/min. Reported dn/dC values for polystyrene (dn/dC = 0.180 mL/g) [41] were used for the molecular weight evaluation of PST macro-CTA. The dn/dC of PDEAEM was determined using a differential refractometer IR Optilab DSP (Wyatt Technology) at 633 nm, 40°C, using nine solutions with concentrations from 0.192 mg/mL to 1.92 mg/mL in THF, obtaining a dn/dC value of 0.087 mL/g.

For the molecular weight calculation of block copolymers, the average dn/dC was calculated from the dn/dC values for the corresponding homopolymers in the blocks and its molar composition (X) determined by NMR using the following equation:

$$\left(\frac{dn}{dC}\right)_{\text{COP}} = X_{\text{PS}}\left(\frac{dn}{dC}\right)_{\text{PST}} + X_{\text{PDEAEM}}\left(\frac{dn}{dC}\right)_{\text{PDEAEM}}. \quad (1)$$

2.4.3. Differential Scanning Calorimetry (DSC). The polymers were dried and purified in vacuum at 40°C to constant weight and their glass transition temperatures (T_g) were obtained on a TA Instrument modulated DSC 2920. Analyses were performed in a helium atmosphere. Samples of 8–12 mg were heated in aluminum pans at a heating rate of 5 K/min in the temperature range from −50°C to 150°C using a temperature modulation of 0.5 K every 60 sec.

2.4.4. Thermogravimetric Analysis (TGA). The decomposition temperatures of the polymers were obtained on a TA Instrument SDT 2920 Simultaneous DSC-TGA thermal analyzer. Analyses were carried out under nitrogen flow. Samples of 10–15 mg were heated in aluminum cups at a heating rate of 10 K/min from room temperature to 700°C. Weight loss and derivative of weight loss are reported.

2.5. Preparation of Thin Films of Block Copolymer. Solutions of PS-*b*-PDEAEM block copolymers (1 wt%) were prepared in toluene or benzene by shaking overnight. Solutions were then spin-coated over freshly cleaved mica using a Laurell Technologies spin coater (model: WS-400B-6NPP/LITE/AS) at spinning velocities of 2000 to 8000 rpm. After spin coating, the thin films formed were dried overnight at ambient temperature.

2.6. Posttreatments of Block Copolymer Thin Films

2.6.1. Thermal Annealing. Some block copolymer films were introduced in a vacuum oven filled with nitrogen gas. A vacuum of 10 torr was achieved and the temperature was set to either 40°C or 90°C. Under such conditions, the films were annealed for different periods of times (24 h up to 80 h). After thermal annealing, the thin films were cooled down to room temperature overnight.

2.6.2. Solvent Annealing. Block copolymer films were introduced in a glass desiccator filled with toluene vapor (26 mmHg). A Petri dish filled with liquid toluene was also introduced in the desiccator to maintain the toluene vapor pressure. The desiccator was closed and maintained at room

temperature (25°C) for different periods of times (24 h up to 80 h). After solvent annealing, the thin films were taken out of the glass desiccator and allowed to dry overnight at ambient temperature.

2.6.3. UV Degradation of Block Copolymer Thin Films. It has been reported that poly(methylmethacrylate) (PMMA) domains can be selectively degraded by UV light irradiation of PS-*b*-PMMA thin films [40–43]. Since PDEAEM is a methacrylate type of polymer, it was tested if these domains could be also degraded using UV light irradiation. Thin films of the block copolymers over different substrates were suspended inside a Rayonet UV reactor with air cooling containing 12 lamps ($\lambda = 254$ nm). UV irradiation was provided for different times. Afterwards, the thin films were washed subsequently with acetic acid to dissolve PDEAEM residues and methanol to eliminate acetic acid residues. After drying at room temperature, the thin films were analyzed.

2.7. Preparation of Block Copolymer Thin Films Containing Gold Nanoparticle. PDEAEM decorated with gold nanoparticles (Au-NP) was prepared as described previously [44]; briefly, PDEAEM (M_n = 18,000 g/mol) was dissolved in water at pH of 4.8 by stirring to yield a 1 mg/mL solution. Afterwards, the Au-NP precursor, tetrachloroauric acid ($HAuCl_4$), was dissolved in the solution and the mixture was heated to 60°C under reflux. 2 mL of a 10 mg/mL solution of the reducing agent tribasic sodium citrate was added dropwise and the reaction was continued at 60°C for 120 min. After cooling, the AuNp product was isolated by increasing the pH of the reaction solution to 9. PDEAEM/AuNP precipitates and it was separated by centrifugation (13,000 rpm). The AuNP product was washed with deionized water, and the clean product was dried in a vacuum oven overnight.

Different amounts of the PDEAEM-AuNP were mixed with the title block copolymer (PS-*b*-PDEAEM), from 0 to 10 wt% relative to block copolymer. These mixtures were dissolved in toluene to achieve a 1 wt% solution by shaking overnight. The solutions containing block copolymer and AuNP were spin-coated as described before.

2.8. Characterization of Block Copolymer Thin Films

2.8.1. Atomic Force Microscopy (AFM). Surface characterization of the thin films was performed by means of a SPM 5100 atomic force microscope (Agilent Technologies) in intermittent mode using silicon cantilevers in the 145 KHz to 160 KHz frequency range using amplitude of 3 to 5 V. The scanner (N9520A) operation interval was 10 μm × 10 μm. Images were edited using the WSxM Develop 3.0 software from electronic nanotechnology [45].

2.8.2. Scanning Transmission Electron Microscopy (STEM). Thin films morphology was studied by STEM. Micrographs were acquired using electron microscope model JEOL JEM-2200-FS working at 200 kV. Images were acquired by bright field and *Z*-contrast detectors. Samples were observed directly without staining due to a reasonable contrast between PDEAEM and PST domains that appear darker compared to PDEAEM. The samples for electron microscope were obtained by detachment of films in hot water ($T = 50$°C). Those film pieces were then suspended on triple distilled water and finally it was picked up over a holey carbon film on a Cu grid of 400 mesh and dried. The average domain size determination was made using DigitalMicrograph software script, and these values were used for basic statistics.

3. Results and Discussion

3.1. Synthesis and Characterization of PS-b-PDEAEM Block Copolymer. The preparation of polystyrene (PS) using the RAFT controlled free-radical polymerization is well established. By adequate selection of a RAFT chain transfer agent (CTA), the ratio of monomer to CTA to initiator determines the obtention of PS in different molecular weights maintaining low polydispersity (PDI = M_n/M_w). In order to use the synthesized PS for block copolymer preparation, it is important to guarantee that the PS is functionalized with the CTA moiety building a macro-CTA and also to guarantee that the CTA moiety is active in the polymerization of the second monomer, which is *N,N′*-diethylaminoethyl methacrylate (DEAEM) in our case. In this study, a trithiocarbonate type of CTA was used since it is reported that trithiocarbonates can be used in the RAFT polymerization of PS [46] and the specific CTA used in this work works well in RAFT polymerization of methacrylates [47]. Table 1 summarizes the results obtained in the synthesis of block copolymers. The first 3 rows show the characteristics of the PS macro-CTAs used in block copolymer preparation. The polydispersities are very low and the obtained molecular weights match well the theoretical values. The fourth row of Table 1 shows the feeding ratios used for the block copolymer synthesis. Again, the polydispersities are low, and the obtained molecular weights demonstrate that the PS-macro-CTAs grew into the desired PS-*b*-PDEAEM products. Figure 1 shows an example of chromatograms (GPC traces) where a macro-CTA is compared with the block copolymer product. The peaks are narrow and the retention times decreased for the block copolymer since in GPC high molecular weights are observed at lower retention times due to the separation technique used.

The composition of the obtained block copolymers was determined by means of ^{1}H-NMR (Figure 2).

For this purpose, the integration of signals at a chemical shift of 4.1 ppm corresponding to two methylene protons of the DEAEM units attached to oxygen was compared to the integration of five aromatic protons of styrene units with signals in the range from 6.3 to 7.3 ppm. A simple calculation shows that the block copolymer depicted in the NMR spectrum on Figure 2 contains 70.7 mol% of styrene and 29.3 mol% of DEAEM units.

Thermal analysis of the block copolymers was undertaken to determine adequate temperatures for thermal annealing of the films of block copolymers. Figure 3 shows the results. In the case of calorimetry (Figure 3(a)), two distinct glass transition temperatures (T_g) are observed, one at −4.9°C corresponding presumably to the poly-DEAEM units and

Table 1: Characteristics of block copolymers.

Macro-CTA	First block			Block copolymer				
	M_n g/mol	PDI[a]	$[M]_0 : [PS] : [I]_0$	M_n g/mol	PDI[a]	Yield[b]	f_{PS}[c]	f'_{PS}[d]
Polystyrene	37,090	1.02	84 : 1 : 0.11	45,760	1.09	56	0.91	0.85
Polystyrene	37,090	1.02	356 : 1 : 0.20	71,980	1.17	53	0.71	0.58
Polystyrene	24,870	1.09	545 : 1 : 0.19	76,280	1.15	51	0.60	0.46

[a]PDI = M_w/M_n; [b]by mass of recovered polymer; [c]molar fraction of PS by ^{1}H-NMR; [d]mass fraction of PS based on f_{PS}.

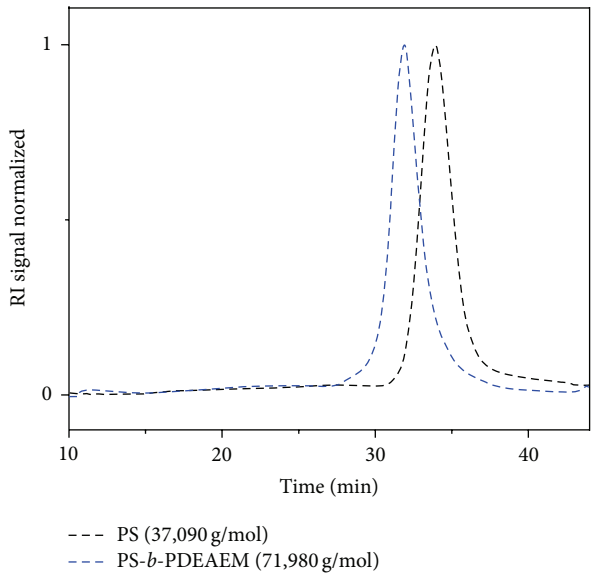

Figure 1: GPC traces of a PS-macro-CTA (M_n = 37,090 g/mol) and the block copolymer (M_n = 71,980 g/mol) prepared from it.

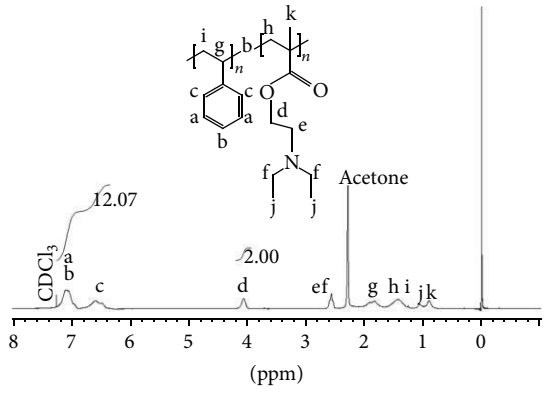

Figure 2: ^{1}H-NMR spectrum of a PS-*b*-PDEAEM block copolymer (M_n = 71,980 g/mol).

the second one at 99.7°C corresponding well to the reported values for PS. In the case of thermogravimetry (Figure 3(b)), thermogram shows that the block copolymer is thermally stable up to 220°C.

These results teach us that, at room temperature, the PDEAEM units are viscoelastic and that, in order to move the PS units, temperature above 105°C is needed. A temperature limit of 200°C can be established as the highest temperature to anneal this block copolymer without degradation.

In addition to these facts, the calorimetry further confirms that the block copolymer consists of immiscible blocks since two separate T_g's are observed. Furthermore, thermogravimetric analysis shows thermal decomposition in two steps: in the first step, parts of PDEAEM are detached, while in the second step, both PDEAEM residual polymer and PS are decomposed.

Results of other block copolymers that were prepared can be consulted in a supplementary results file (see Supplementary Material available online at http://dx.doi.org/10.1155/2014/725356).

3.2. Towards Equilibrium Ordering of PS-b-PDEAEM Thin Films. Given the composition of the block copolymers prepared, we decided to study in deep the block copolymer containing 60 mol% PS (46 mass%) with a molecular weight of 76 280 g/mol. This block copolymer is expected to form at thermodynamic equilibrium lamellae; however, a gyroid nanostructure is also a possibility. As for solvents, toluene, benzene, and tetrahydrofuran (THF) were chosen due to the Flory-Huggins polymer-solvent (P-S) interaction parameters ($\chi_{P\text{-}S}$) calculated with PS and PDEAEM, namely, 0.347 and 0.350 for toluene, 0.341 and 0.380 for benzene, and 0.34 and 0.36 for THF, values that are very similar to both polymers indicating that in this solvent there is only a slight or not a solvating preference for one of the blocks. These parameters were calculated according to (2) [48] using the solubility parameters (δ) reported in the literature [49] at room temperature (298.15 K), with the exception of that of PDEAEM estimated from the Hoy theory of group contributions [50] to be δ_{PDEAEM} = 17.7 $(MPa)^{1/2}$. For polystyrene the value used is δ_{PS} = 18.6 $(MPa)^{1/2}$. Consider

$$\chi_{P\text{-}S} = \frac{V_S}{RT}\left(\delta_S - \delta_P\right)^2 + 0.34. \quad (2)$$

V_S is the molar volume of the solvent, R is the universal gas constant, and T is the temperature.

Simple solubility tests showed that the best solubility for both types of homopolymers was given by THF. Nevertheless, this solvent was discarded due to the high vapor pressure of the solvent that resulted in film detachment and void formation in the films. The following results make use of toluene and benzene as selected solvents, even if the solubility of PDEAEM is worse than that of PS in those solvents.

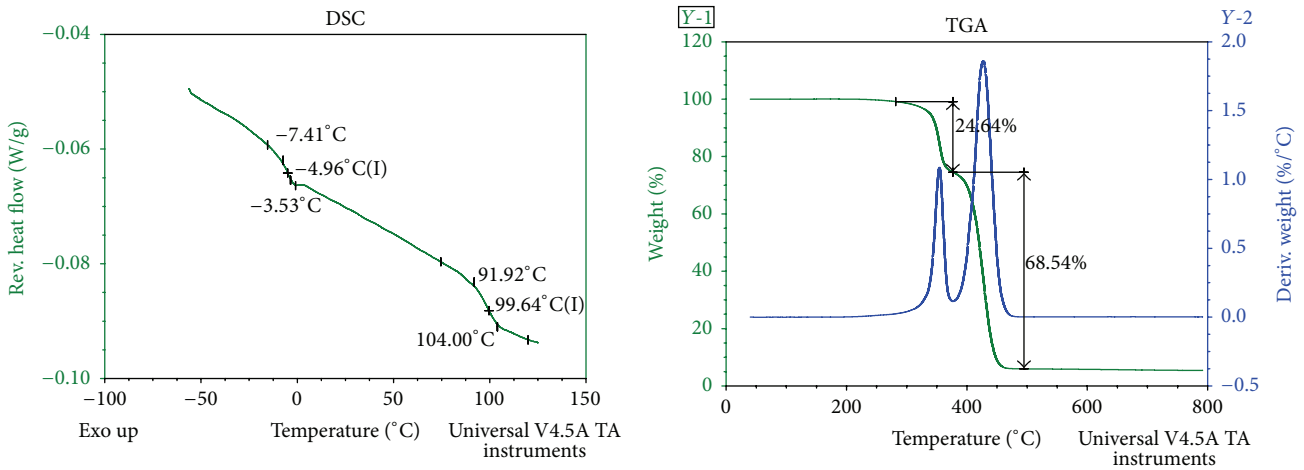

Figure 3: Thermograms by DSC (a) and TGA (b) of a PS-*b*-PDEAEM block copolymer (M_n = 71,980 g/mol).

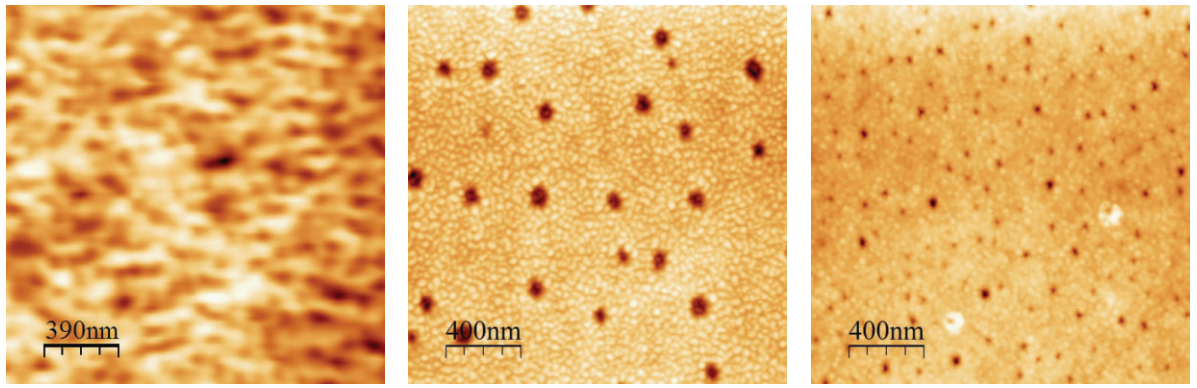

Figure 4: AFM topographic images obtained using the intermittent contact mode of $PSt_{60\%}$-*b*-$PDEAEM_{40\%}$ thin films prepared from a 1% w/w toluene solution over mica substrate as a function of spin coating velocity: (a) 2000 rpm; (b) 5000 rpm; and (c) 8000 rpm.

Figure 4 shows thin films prepared from toluene solutions over mica substrate at room temperature (25°C) as a function of spin coating velocity. It is clear that no equilibrium structure is formed and that a spinning velocity of 5000 to 8000 rpm seems to favor phase segregation.

Figure 5 shows AFM images of thin films prepared using the same polymer but in solution in benzene over freshly cleaved mica substrate.

In this case, a constant spinning velocity was used and thermal annealing at a relatively low temperature was applied to gain movement of PDEAEM units in the block copolymer that resulted in a transition from elongated type of aggregates right after spin coating to a phase separated nanostructure. Results show that after 36 h of moderate thermal annealing (40°C) a knitted pattern resembling a bicontinuous gyroid nanostructure was obtained. However, longer annealing time destroyed this nanostructure.

Figure 6 shows AFM images from the same block copolymer deposited over mica substrate, but in this case by using toluene solution for the start and at constant spinning velocity of 8000 rpm. In this case, the annealing temperature was risen to 90°C, a temperature at 10 torr at which the movements of both PDEAEM and slightly for PS units in the block copolymer were expected. Results show that, after 40 h of thermal annealing, the same knitted nanostructure was found in this case as for thin films prepared from benzene solutions after annealing at 40°C. The best order was found after 90 h of thermal annealing; however, the main features can be observed already after 40 h.

Up to these results, it looked like a bicontinuos (gyroid) nanostructure was the equilibrium self-assembled one for this specific block copolymer; however, solvent annealing proved to us that we were wrong. Figure 7 shows AFM images of solvent-annealed nanostructures obtained from the $PS_{60\%}$-*b*-$PDEAEM_{40\%}$ block copolymer deposited by spin coating over mica substrate. Images clearly show that solvent annealing in toluene at 25°C for extended periods of time (80 h) resulted in the most expected equilibrium lamellar

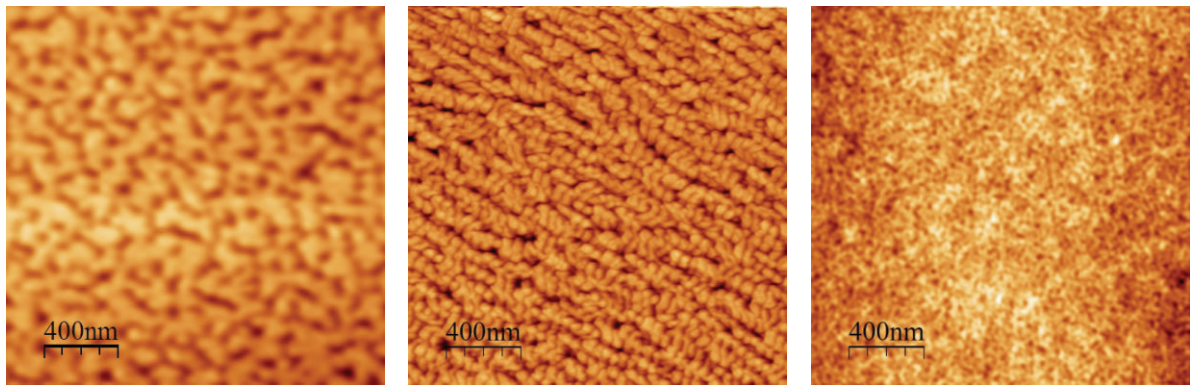

FIGURE 5: AFM topographic images obtained using the intermittent contact mode of $PSt_{60\%}$-*b*-$PDEAEM_{40\%}$ thin films prepared from a 1% w/w benzene solution over mica substrate at a spinning velocity of 5000 rpm: (a) directly after spin coating (25°C) and after annealing in vacuum (10 torr) at 40°C for (b) 36 h and (c) 48 h.

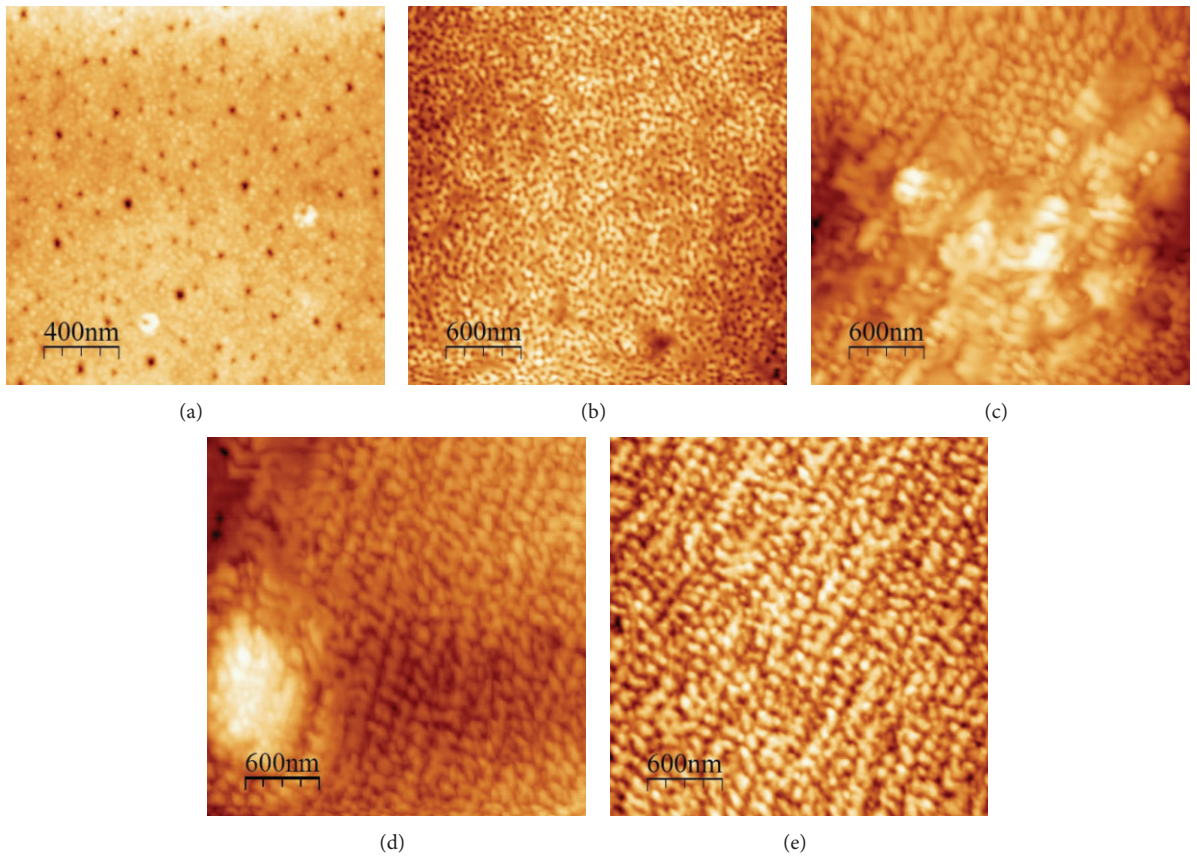

FIGURE 6: AFM topographic images obtained using the intermittent contact mode of $PSt_{60\%}$-*b*-$PDEAEM_{40\%}$ thin films prepared from a 1% w/w toluene solution over mica substrate at a spinning velocity of 8000 rpm: (a) directly after spin coating (25°C) and after annealing in vacuum (10 torr) at 90°C for (b) 20 h, (c) 40 h, (d), 60 h, and (e) 90 h.

nanostructures. It is also clear that from toluene solution the direct spin-coated films show micelle-like features and that only after prolonged solvent annealing treatment, the equilibrium nanostructures are formed.

To confirm the lamellar nanoordering, polymer film was detached from the mica substrate with hot water, and the thin film was studied using scanning transmission electron microscopy (STEM).

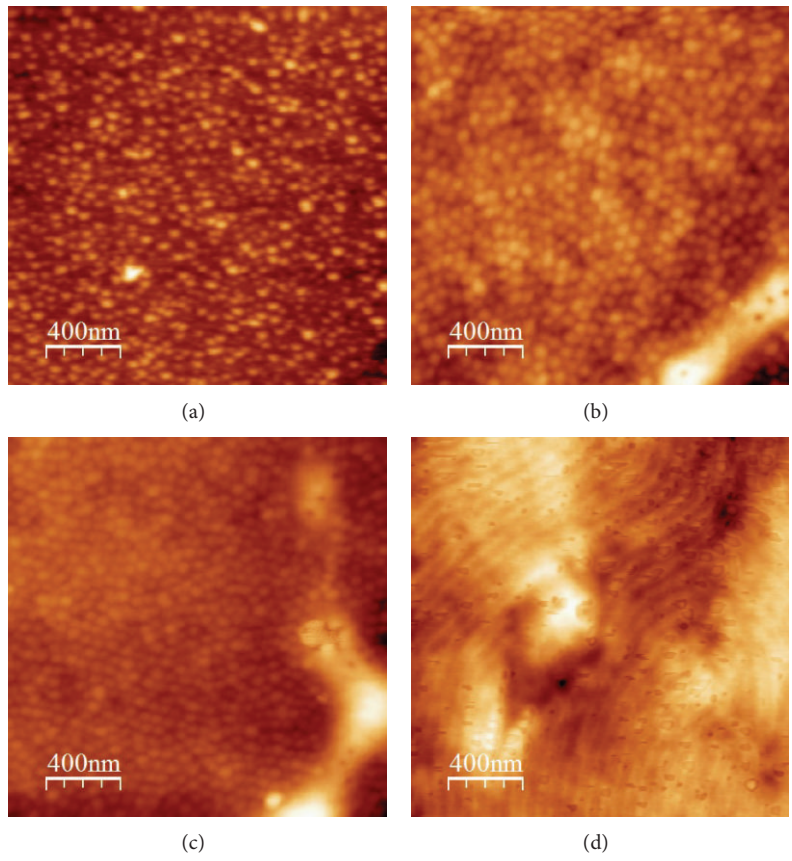

Figure 7: AFM topographic images obtained using the intermittent contact mode of $PSt_{60\%}$-*b*-$PDEAEM_{40\%}$ thin films prepared from a 1% w/w toluene solution over mica substrate at a spinning velocity of 5000 rpm: (a) directly after spin coating (25°C) and after annealing in a toluene vapor chamber (760 torr, 25°C) for (b) 24 h, (c) 36 h, and (d) 80 h.

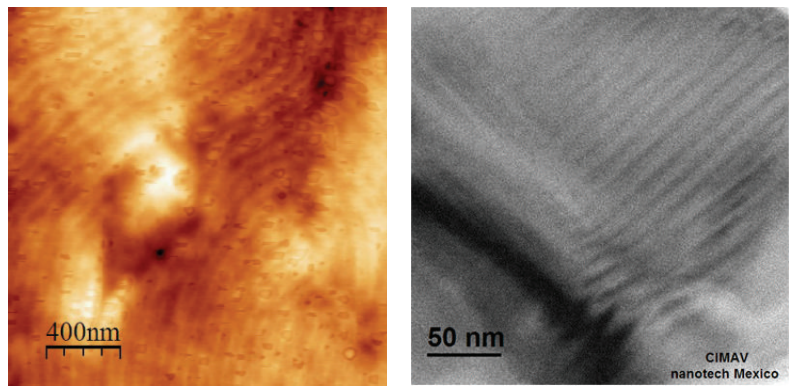

Figure 8: Images of $PSt_{60\%}$-*b*-$PDEAEM_{40\%}$ thin films prepared using a 1% w/w toluene solution over mica substrate at a spinning velocity of 5000 rpm and annealed for 80 h with toluene vapor at 25°C: (a) AFM topographic image obtained using the intermittent contact mode and (b) STEM image (*Z*-contrast) obtained from detached film.

Figure 8 compares STEM images with AFM images for the thin films prepared confirming the lamellae nanopatterns. The lamellae were measured from AFM and STEM images giving the following results (see statistics in Supplementary Material). In the case of AFM, the average diameter of a (light yellow) lamella is 51.5±3.7 nm, while the interlamellar distance is 73.6 ± 6.8 nm; in the case of STEM image, 8.5 ± 0.95 nm is an average diameter of the pale gray lamellae (PDEAEM phase) and 5.5 ± 0.77 nm for the dark grey lamellae (PS-phase); and the interlamellar distance is

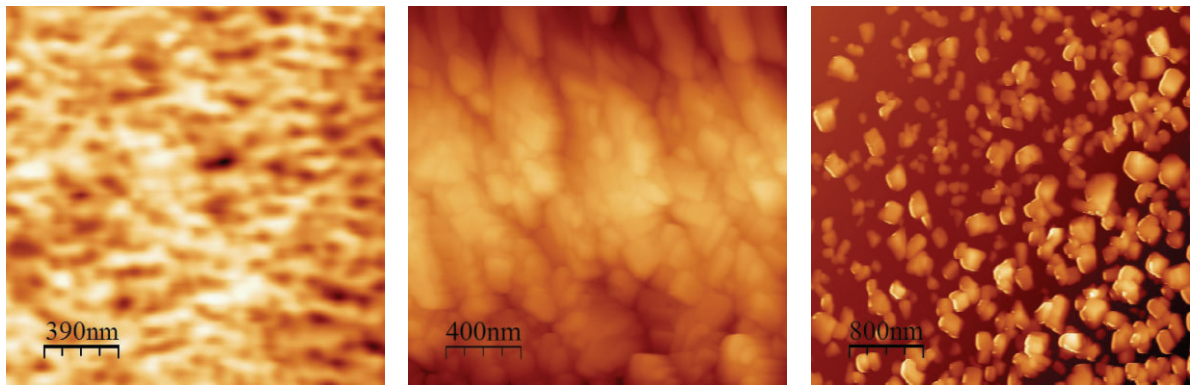

(a) (b) (c)

FIGURE 9: AFM topographic images obtained using the intermittent contact mode of $PSt_{60\%}$-*b*-$PDEAEM_{40\%}$ thin films prepared from a 1% w/w toluene solution over mica substrate at a spinning velocity of 2000 rpm: (a) directly after spin coating (25°C) and after thermal annealing in vacuum (10 torr, 170°C) for (b) 120 h and (c) 138 h.

13.46 ± 1.27 nm. Given the molecular weight of the block copolymer (76,280 g/mol), the content, and molecular weights of both comonomers, we can calculate that the number of repetitive units is as the following: $PS_{(n=239)}$-*b*-$PDEAEM_{(m=278)}$. If the block copolymer would be an extended chain, its maximal size would be 517 times the contribution of a monomer unit based on tetrahedral C–C bond (0.254 nm [51]), namely, 131.3 nm. However, polymer chains are coiled, even if dispersed in a good solvent. For example, for PS in tetrahydrofuran (THF), the relationship between molecular weight and radius of gyration (R_g) is described by the following equation (3) [52]:

$$R_g\,(\text{Å}) = (0.2092)\,M_w^{0.56}. \tag{3}$$

If we consider the whole block copolymer constituted of styrene units (517 units), its molecular weight would be close to 54000 g/mol, which would yield a R_g of 9.3 nm only. The end to end distance (extension *h*) of a coiled polymer chain in a good solvent can be estimated by the following simple equation [53]:

$$h^2 = 7.04R_g^2. \tag{4}$$

In our case, *h* would be 24.7 nm. Therefore, domains between 25 nm and 130 nm are to be expected in self-assembled films of the studied $PS_{60\%}$-*b*-$PDEAEM_{40\%}$. The lamellae observed by AFM are in between the calculated sizes, while the STEM image shows smaller domains, possibly by shrinkage as a side effect of film detaching and drying procedures.

3.3. Nonequilibrium Ordering of PS-b-PDEAEM Thin Film. The fact that the $PSt_{60\%}$-*b*-$PDEAEM_{40\%}$ block copolymer formed gyroid-like patterns under certain conditions as a nonequilibrium nanostructure opened the possibility to study which other nanostructures are possible to obtain using this block copolymer in a reproducible way.

In the following text, case examples are presented which show the richness of nanostructures that can be produced using this block copolymer.

Figure 9 shows what happens if a not very thin film of the title block copolymer is prepared and annealed at a relatively high temperature of 170°C (where both blocks are freely mobile). The polymer film is detached from the mica substrate to form "nanoflakes" of an average size of 193.5 ± 73.4 nm (Figure 9(c)).

Another case consisted in UV irradiation treatment of $PSt_{60\%}$-*b*-$PDEAEM_{40\%}$ thin films prepared at 5000 rpm. Figure 10 shows AFM images of the thin film directly after spin coating compared to the film after irradiation with UV light (λ = 254 nm) for different periods of time. Results show that partial degradation occurred, presumably partial depolymerization of the PDEAEM phase leading to a rough surface. RMS values increased from 1.09 nm (Figure 10(a)) directly after spin coating to 3.53 nm after irradiation for 15 min (Figure 10(b)) and to 4.07 nm after irradiation for 30 min (Figure 10(c)). Degradation of polymethacrylate domains by UV irradiation is well known and served as a method to generate nanotemplates [42, 54]. This study demonstrates that nanopatterns can be generated fast (spin coating + 15 min UV irradiation) using PS-*b*-PDEAEM as template; however, no regularly ordered nanostructure can be achieved that fast.

It has been reported that the ordered nanostructures formed by block copolymers can be altered by mixing them with homopolymers, enriching one of the phases [55], or by mixing them with nanoparticles that may show specific interactions with one of the two blocks [56]. In this study, we used a linear PDEAEM (M_n = 18,000 g/mol) that already contains gold nanoparticles (AuNPs) of an average size of 7.5 nm to study nanostructure modification of $PSt_{60\%}$-*b*-$PDEAEM_{40\%}$.

Figure 11 shows results on thin films prepared using 10 w% of the AuNPs containing PDEAEM and 90 w% of the title block copolymer. Images taken at 25°C directly after spin coating showed that there is no significant difference to the previously studied thin films with block copolymer only. However, thermal annealing at 90°C showed a substantial difference as compared with thin films prepared of block copolymers only. While the title block copolymer forms

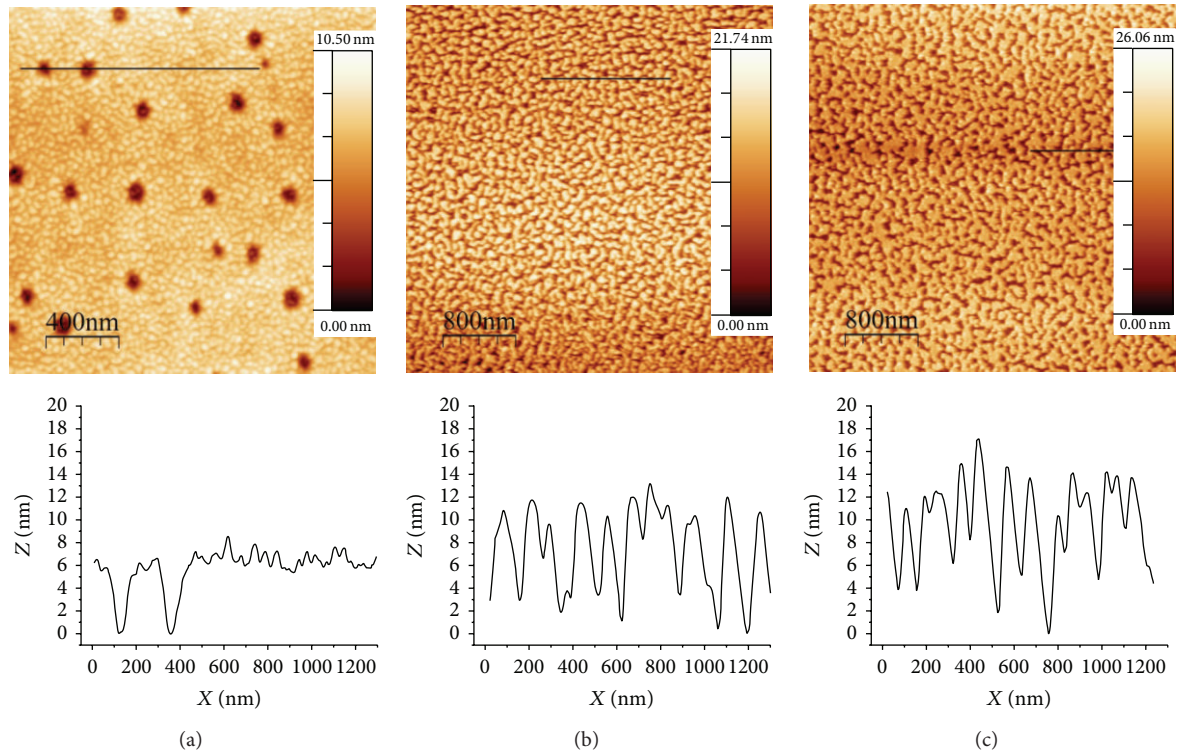

FIGURE 10: AFM topographic images obtained using the intermittent contact mode of $PSt_{60\%}$-*b*-$PDEAEM_{40\%}$ thin films prepared from a 1% w/w toluene solution over mica substrate at a spinning velocity of 5000 rpm: (a) directly after spin coating (RMS = 1.09 nm) and after UV irradiation (λ = 254 nm) for different times: (b) 15 min (RMS = 3.53 nm) and (c) 30 min (RMS = 4.07 nm).

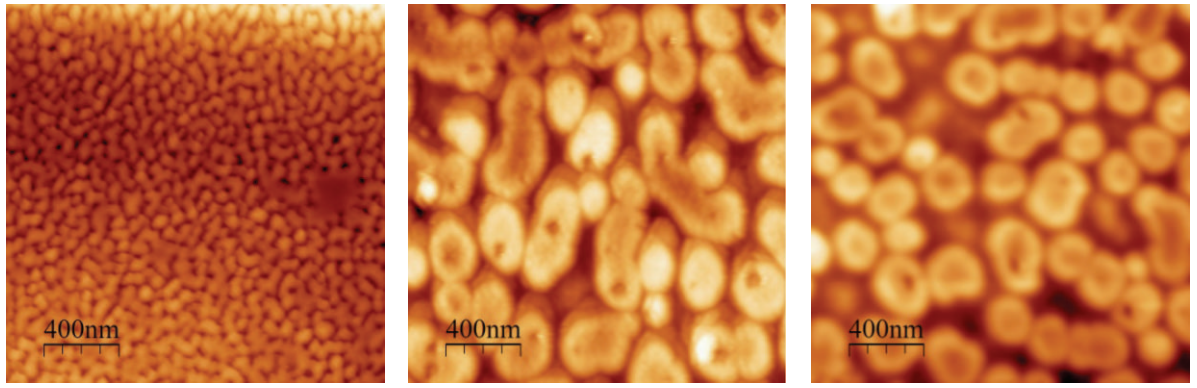

FIGURE 11: AFM topographic images obtained using the intermittent contact mode of $PSt_{60\%}$-*b*-$PDEAEM_{40\%}$/PDEAEM-AuNP (9 : 1) thin films prepared from a 1% w/w toluene solution over mica substrate at a spinning velocity of 8000 rpm: (a) directly after spin coating (25°C) and after annealing in vacuum (10 torr) at 90°C for (b) 24 h and (c) 48 h.

a bicontinuous (gyroid like) phase, the mixture with PDEAEM-AuNP forms micelle-like nanostructures with voids in the middle. A similar nanostructure is reported already with the name of toroids [57, 58]. After 48 h annealing time, the micellar nanostructures are kept. From the images in Figure 11, there is no clear evidence where PDEAEM-AuNPs are located. What we can expect is that AuNPs are located in vicinity of PDEAEM units since tertiary amine groups interact strongly with AuNPs.

Electron microscope images obtained by STEM mode show the uniform size and homogeneous distribution of AuNPs. Figures 12(a) and 12(b) show a comparison between AFM image and STEM. In both images, a similar morphology after the sample was detached from the mica substrate can

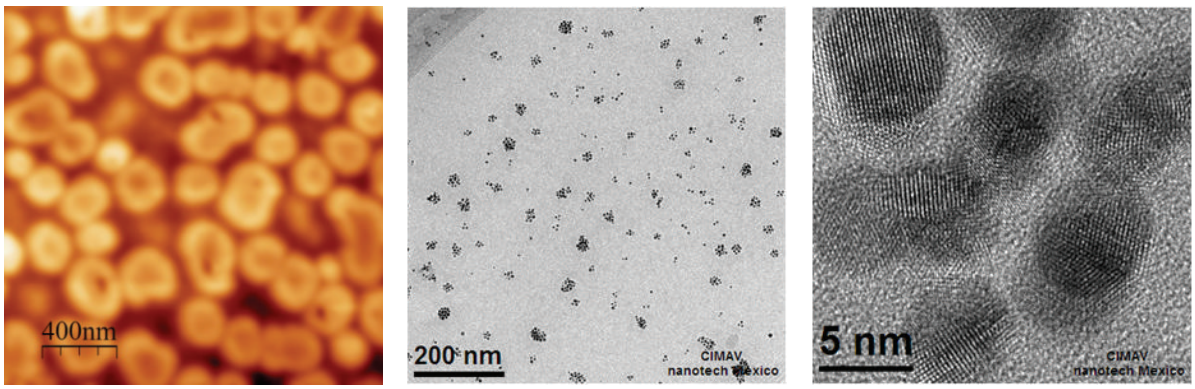

(a) (b) (c)

FIGURE 12: Images of $PSt_{60\%}$-*b*-$PDEAEM_{40\%}$/PDEAEM-AuNP (9 : 1) thin films prepared using a 1% w/w toluene solution over mica substrate at a spinning velocity of 8000 rpm after annealing in vacuum at 90°C for 48 h: (a) AFM topographic image obtained using the intermittent contact mode, (b) STEM low magnification image, obtained from detached film, and (c) higher magnification image of a cluster of AuNPs from image shown in (b).

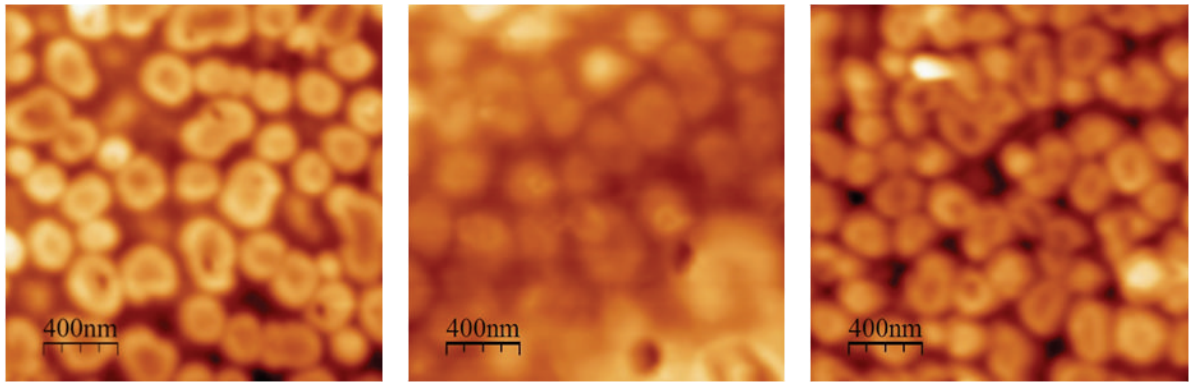

(a) (b) (c)

FIGURE 13: AFM topographic images obtained using the intermittent contact mode of $PSt_{60\%}$-*b*-$PDEAEM_{40\%}$/PDEAEM-AuNP (9 : 1) thin films prepared from a 1% w/w toluene solution over mica substrate at a spinning velocity of 8000 rpm after different treatment methods: (a) after annealing in vacuum (10 torr) at 90°C for 48 h; (b) after annealing in a THF vapor chamber (760 torr, 25°C) for 24 h; and (c) after UV irradiation (λ = 254 nm) by 20 min.

be seen. The tiny dark spots represent the AuNPs, which are dispersed homogeneously in arrays. These images show that PDEAEM-AuNPs are located in the middle part of the micelle-like toroidal nanostructres formed (Figure 12(b)). Therefore, we postulate that PS domains form the outer layer of the micelles and PDEAEM phase forms the internal part, resembling the core-shell morphology.

From the images the diameter of these spherical nanodomains was measured and an average of 261 ± 14.5 nm was calculated as diameter of the micelles, formed by a core of 99.5 ± 31.9 nm and a shell of variable thickness. Figure 12(c) shows bright field image at higher magnification, evidencing that these gold NPs are crystalline and all of them show d-spaces which belong to metallic gold. The morphology obtained by using PDEAEM-AuNP is interesting since it tends to form micelles with voids in the middle that can be used to position AuNPs in a controlled way over a surface.

Given these results, we decide to test if this morphology was achievable by other treatment methods. This was important, since in the case of polystyrene-*block*-poly(4-vinylpyridine) it was reported that the formation of toroids was only achievable at specific strong acidic conditions [57] or only in a combination of a specific surface (gold or substrate with nitrided layer) and annealing with high polarity solvents like ethanol and methanol [58]. Figure 13 shows that the formation of toroidal morphology is robust, since it can be obtained by using at least three different methods: thermal treatment, solvent annealing, and also irradiation with UV light. In the latter case, the size of the toroids is similar to that obtained by thermal annealing: diameter of 268 ± 36 nm with 87.5 ± 1.7 nm core. These results show that the title block copolymer can be combined with PDEAEM attached to nanoparticles to create an ordered surface where nanoparticles may be deposited in an ordered manner.

4. Conclusions

A series of poly(styrene)-*b*-poly(*N,N′*-diethylaminoethyl methacrylate) block copolymers can be prepared controlling size and composition by using RAFT free-radical polymerization starting with a PS block; polydispersities were low (<1.2).

Thin films of $PS_{60\%}$-*b*-$PDEAEM_{40\%}$ block copolymer deposited over mica substrates form a lamellar nanostructure at equilibrium. This was achievable only after solvent annealing (toluene) for extended periods of time (80 h).

Thin films of $PS_{60\%}$-*b*-$PDEAEM_{40\%}$ block copolymer deposited over mica substrates form several nonequilibrium nanostructures that are reproducible: a knitted bicontinuous nanostructure by thermal annealing in vacuum at 90°C, a porous nanotemplate direct after spin coating and UV irradiation for short time (15 min), and toroidal self-assembled nanostructures with PS shell and PDEAEM core when the title block copolymer is mixed with a linear PDEAEM attached to gold nanoparticles.

$PS_{60\%}$-*b*-$PDEAEM_{40\%}$ block copolymer can be combined with PDEAEM attached to gold nanoparticles to create an ordered surface where nanoparticles may be deposited in an ordered way. This is achievable, fast, and easy by using, for example, UV irradiation. This approach may be extended to other types of nanoparticles.

Additional AFM images can be found in the Supplementary Material file described before.

Conflict of Interests

The authors declare that there is no conflict of interests regarding the publication of this paper.

Acknowledgments

This investigation was financed by a grant from the National Council of Science and Technology of Mexico (CONACYT no. SEP2007-60792). The authors acknowledge the National Nanoscience and Nanotechnology Network of Mexico for supporting Pedro Navarro-Vega for a research stay at CIMAV. They thank A. Ochoa and I. A. Rivero from IT Tijuana for performing NMR analysis. They also thank C. Ornelas, W. Antunez, and L. De la Torre for their help at CIMAV.

References

[1] J. N. L. Albert and T. H. Epps III, "Self-assembly of block copolymer thin films," *Materials Today*, vol. 13, no. 6, pp. 24–33, 2010.

[2] D. H. Lee, H. Cho, S. Yoo, and S. Park, "Ordering evolution of block copolymer thin films upon solvent-annealing process," *Journal of Colloid and Interface Science*, vol. 383, no. 1, pp. 118–123, 2012.

[3] M. W. Matsen and F. S. Bates, "Conformationally asymmetric block copolymers," *Journal of Polymer Science, Part B: Polymer Physics*, vol. 35, no. 6, pp. 945–952, 1997.

[4] U. Jeong, H.-C. Kim, R. L. Rodriguez et al., "Asymmetric block copolymers with homopolymers: routes to multiple length scale nanostructures," *Advanced Materials*, vol. 14, no. 4, pp. 274–276, 2002.

[5] J.-Y. Wang, W. Chen, J. D. Sievert, and T. P. Russell, "Lamellae orientation in block copolymer films with ionic complexes," *Langmuir*, vol. 24, no. 7, pp. 3545–3550, 2008.

[6] T. G. Fitzgerald, R. A. Farrell, N. Petkov et al., "Study on the combined effects of solvent evaporation and polymer flow upon block copolymer self-assembly and alignment on topographic patterns," *Langmuir*, vol. 25, no. 23, pp. 13551–13560, 2009.

[7] Y. Li, H. Huang, T. He, and Y. Gong, "Solvent vapor induced morphology transition in thin film of cylinder forming diblock copolymer," *Applied Surface Science*, vol. 257, no. 18, pp. 8093–8101, 2011.

[8] R. Guo, H. Huang, B. Du, and T. He, "Solvent-induced morphology of the binary mixture of diblock copolymer in thin film: the block length and composition dependence of morphology," *The Journal of Physical Chemistry B*, vol. 113, no. 9, pp. 2712–2724, 2009.

[9] S. W. Hong and T. P. Russell, "Block copolymer thin films," in *Polymer Science: A Comprehensive Reference*, K. Matyjaszewski and M. Möller, Eds., vol. 7, pp. 45–69, Elsevier B.V., Amsterdam, The Netherlands, 2012.

[10] J. Bang, B. J. Kim, G. E. Stein et al., "Effect of humidity on the ordering of PEO-based copolymer thin films," *Macromolecules*, vol. 40, no. 19, pp. 7019–7025, 2007.

[11] M. Yoo, S. Kim, S. G. Jang et al., "Controlling the orientation of block copolymer thin films using thermally-stable gold nanoparticles with tuned surface chemistry," *Macromolecules*, vol. 44, no. 23, pp. 9356–9365, 2011.

[12] H.-C. Kim, S.-M. Park, W. D. Hinsberg, and I. R. Division, "Block copolymer based nanostructures: materials, processes, and applications to electronics," *Chemical Reviews*, vol. 110, no. 1, pp. 146–177, 2010.

[13] H. Wang, A. B. Djurišić, M. H. Xie, W. K. Chan, and O. Kutsay, "Perpendicular domains in poly(styrene-*b*-methyl methacrylate) block copolymer films on preferential surfaces," *Thin Solid Films*, vol. 488, no. 1-2, pp. 329–336, 2005.

[14] E. Buck and J. Fuhrmann, "Surface-induced microphase separation in spin-cast ultrathin diblock copolymer films on silicon substrate before and after annealing," *Macromolecules*, vol. 34, no. 7, pp. 2172–2178, 2001.

[15] D. A. Olson, L. Chen, and M. A. Hillmyer, "Templating nanoporous polymers with ordered block copolymers," *Chemistry of Materials*, vol. 20, no. 3, pp. 869–890, 2008.

[16] M. Radjabian, J. Koll, K. Buhr, U. A. Handge, and V. Abetz, "Hollow fiber spinning of block copolymers: influence of spinning conditions on morphological properties," *Polymer*, vol. 54, no. 7, pp. 1803–1812, 2013.

[17] S. Park, J.-Y. Wang, B. Kim, J. Xu, and T. P. Russell, "A simple route to highly oriented and ordered nanoporous block copolymer templates," *ACS Nano*, vol. 2, no. 4, pp. 766–772, 2008.

[18] C. Wang, S. Yang, J. Xu, and M. Zhu, "Morphology transformation of polystyrene-block-poly(ethylene oxide) vesicle on surface," *Polymer*, vol. 54, no. 14, pp. 3709–3715, 2013.

[19] W. Van Zoelen, T. Asumaa, J. Ruokolainen, O. Ikkala, and G. Ten Brinke, "Phase behavior of solvent vapor annealed thin films of PS-b-P4VP(PDP) supramolecules," *Macromolecules*, vol. 41, no. 9, pp. 3199–3208, 2008.

[20] I. Zalakain, N. Politakos, R. Fernandez et al., "Morphology response by solvent and vapour annealing using polystyrene/poly(methyl methacrylate) brushes," *Thin Solid Films*, vol. 539, pp. 201–206, 2013.

[21] S. E. Mastroianni and T. H. Epps, "Interfacial manipulations: controlling nanoscale assembly in bulk, thin film, and solution block copolymer systems," *Langmuir*, vol. 29, no. 12, pp. 3864–3878, 2013.

[22] A. Nunns, J. Gwyther, and I. Manners, "Inorganic block copolymer lithography," *Polymer*, vol. 54, no. 4, pp. 1269–1284, 2013.

[23] C. Sinturel, M. Vayer, M. Morris, and M. A. Hillmyer, "Solvent vapor annealing of block polymer thin films," *Macromolecules*, vol. 46, no. 14, pp. 5399–5415, 2013.

[24] C. Park, J. Yoon, and E. L. Thomas, "Enabling nanotechnology with self assembled block copolymer patterns," *Polymer*, vol. 44, no. 22, pp. 6725–6760, 2003.

[25] W.-N. He and J.-T. Xu, "Crystallization assisted self-assembly of semicrystalline block copolymers," *Progress in Polymer Science*, vol. 37, no. 10, pp. 1350–1400, 2012.

[26] S. O'Driscoll, G. Demirel, R. A. Farrell et al., "The morphology and structure of PS-b-P4VP block copolymer films by solvent annealing: effect of the solvent parameter," *Polymers for Advanced Technologies*, vol. 22, no. 6, pp. 915–923, 2011.

[27] S. P. Paradiso, K. T. Delaney, C. J. García-Cervera, H. D. Ceniceros, and G. H. Fredrickson, "Block copolymer self assembly during rapid solvent evaporation: Insights into cylinder growth and stability," *ACS Macro Letters*, vol. 3, no. 1, pp. 16–20, 2014.

[28] P. Mokarian-Tabari, T. W. Collins, J. D. Holmes, and M. A. Morris, "Cyclical "flipping" of morphology in block copolymer thin films," *ACS Nano*, vol. 5, no. 6, pp. 4617–4623, 2011.

[29] S. Y. Choi, C. Lee, J. W. Lee, C. Park, and S. H. Kim, "Dewetting-induced hierarchical patterns in block copolymer films," *Macromolecules*, vol. 45, no. 3, pp. 1492–1498, 2012.

[30] Y. S. Jung and C. A. Ross, "Orientation-controlled self-assembled nanolithography using a polystyrene-polydimethylsiloxane block copolymer," *Nano Letters*, vol. 7, no. 7, pp. 2046–2050, 2007.

[31] L. Xue and Y. Han, "Pattern formation by dewetting of polymer thin film," *Progress in Polymer Science*, vol. 36, no. 2, pp. 269–293, 2011.

[32] B. Bharatiya, J.-M. Schumers, E. Poggi, and J.-F. Gohy, "Supramolecular assemblies from poly(styrene)-block-poly(4-vinylpyridine) diblock copolymers mixed with 6-Hydroxy-2-naphthoic acid," *Polymers*, vol. 5, no. 2, pp. 679–695, 2013.

[33] I. Tokarev, R. Krenek, Y. Burkov et al., "Microphase separation in thin films of poly(styrene-*block*-4-vinylpyridine) copolymer-2-(4'-hydroxybenzeneazo)benzoic acid assembly," *Macromolecules*, vol. 38, no. 2, pp. 507–516, 2005.

[34] A. Sidorenko, I. Tokarev, S. Minko, and M. Stamm, "Ordered reactive nanomembranes/nanotemplates from thin films of block copolymer supramolecular assembly," *Journal of the American Chemical Society*, vol. 125, no. 40, pp. 12211–12216, 2003.

[35] M. Böhme, B. Kuila, H. Schlörb, B. Nandan, and M. Stamm, "Thin films of block copolymer supramolecular assemblies: microphase separation and nanofabrication," *Physica Status Solidi (B)*, vol. 247, no. 10, pp. 2458–2469, 2010.

[36] B. Nandan, M. K. Vyas, M. Bohme, and M. Stamm, "Composition-dependent morphological transitions and pathways in switching of fine structure in thin films of block copolymer supramolecular assemblies," *Macromolecules*, vol. 43, no. 5, pp. 2463–2473, 2010.

[37] A. Bousquet, E. Ibarboure, E. Papon, C. Labrugère, and J. Rodríguez-Hernández, "Structured multistimuli-responsive functional polymer surfaces obtained by interfacial diffusion of amphiphilic block copolymers," *Journal of Polymer Science Part A: Polymer Chemistry*, vol. 48, no. 9, pp. 1952–1961, 2010.

[38] C. S. Patrickios, W. R. Hertler, N. L. Abbott, and T. A. Hatton, "Diblock, ABC triblock, and random methacrylic polyampholytes: synthesis by group transfer polymerization and solution behavior," *Macromolecules*, vol. 27, no. 4, pp. 930–937, 1994.

[39] A. S. Lee, A. P. Gast, V. Bütün, and S. P. Armes, "Characterizing the structure of pH dependent polyelectrolyte block copolymer micelles," *Macromolecules*, vol. 32, no. 13, pp. 4302–4310, 1999.

[40] S. H. Thang, B. Y. K. Chong, R. T. A. Mayadunne, G. Moad, and E. Rizzardo, "A novel synthesis of functional dithioesters, dithiocarbamates, xanthates and trithiocarbonates," *Tetrahedron Letters*, vol. 40, no. 12, pp. 2435–2438, 1999.

[41] J. Brandrup and E. H. Immergut, *Polymer Handbook*, Wiley-Interscience, New York, NY, USA, 3rd edition, 1989.

[42] A. J. Hong, C.-C. Liu, Y. Wang et al., "Metal nanodot memory by self-assembled block copolymer lift-off," *Nano Letters*, vol. 10, no. 1, pp. 224–229, 2010.

[43] T. Kim, S. Wooh, J. G. Son, and K. Char, "Orientation control of block copolymer thin films placed on ordered nanoparticle monolayers," *Macromolecules*, vol. 46, no. 20, pp. 8144–8151, 2013.

[44] N. A. Cortez-Lemus, A. Licea-Claverie, F. Paraguay-Delgado, and G. Alonso-Nuñez, "Controlling the size of gold nanoparticles by using poly(N,N,-diethylaminoethyl methacrylate)," *Journal of Nanoparticle Research*. Under review.

[45] I. Horcas, R. Fernández, J. M. Gómez-Rodríguez, J. Colchero, J. Gómez-Herrero, and A. M. Baro, "WSXM: a software for scanning probe microscopy and a tool for nanotechnology," *Review of Scientific Instruments*, vol. 78, no. 1, Article ID 013705, 2007.

[46] J. Chiefari, R. T. A. Mayadunne, C. L. Moad et al., "Thiocarbonylthio compounds (S=C(Z)S-R) in free radical polymerization with reversible addition-fragmentation chain transfer (RAFT polymerization). Effect of the activating Group Z," *Macromolecules*, vol. 36, no. 7, pp. 2273–2283, 2003.

[47] G. Moad, Y. K. Chong, A. Postma, E. Rizzardo, and S. H. Thang, "Advances in RAFT polymerization: the synthesis of polymers with defined end-groups," *Polymer*, vol. 46, no. 19, pp. 8458–8468, 2005.

[48] J. Brandrup, E. H. Immergut, and E. A. Grulke, *Polymer Handbook*, John Wiley & Sons, New York, NY, USA, 4th edition, 1999.

[49] J. Brandrup, E. H. Immergut, and E. A. Grulke, *Polymer Handbook*, pp. VII/688–VII/707, John Wiley & Sons, New York, NY, USA, 4th edition, 1999.

[50] D. W. van Krevelen, *Properties of Polymers*, Elsevier Science, Amsterdam, The Netherlands, 3rd edition, 1997.

[51] D. Kafouris and C. S. Patrickios, "Synthesis and characterization of shell-cross-linked polymer networks and large-core star polymers: effect of the volume of the cross-linking mixture," *European Polymer Journal*, vol. 45, no. 1, pp. 10–18, 2009.

[52] K. Venkataswamy, A. M. Jamieson, and R. G. Petschek, "Static and dynamic properties of polystyrene in good solvents: ethylbenzene and tetrahydrofuran," *Macromolecules*, vol. 19, no. 1, pp. 124–133, 1986.

[53] K. F. Arndt and G. Müller, *Polymercharakterisierung*, Carl Hanser, München, Germany, 1996.

[54] M. M. Alam, Y.-R. Lee, J.-Y. Kim, and W.-G. Jung, "Fabrication of nanopatterns using block copolymer and controlling surface morphology," *Journal of Colloid and Interface Science*, vol. 348, no. 1, pp. 206–210, 2010.

[55] M. Rosales-Guzmán, R. Alexander-Katz, P. Castillo-Ocampo, A. Vega-Ríos, and A. Licea-Claveríe, "Strain state of poly(*N*-isopropylacrylamide) in polystyrene-*b*-poly(*N*- isopropylacrylamide) block copolymers and binary blends with polystyrene," *Journal of Polymer Science, Part B: Polymer Physics*, vol. 51, no. 18, pp. 1368–1376, 2013.

[56] G.-K. Xu, X.-Q. Feng, and S.-W. Yu, "Controllable nanostructural transitions in grafted nanoparticle-block copolymer composites," *Nano Research*, vol. 3, no. 5, pp. 356–362, 2010.

[57] M. Aizawa and J. M. Buriak, "Block copolymer templated chemistry for the formation of metallic nanoparticle arrays on semiconductor surfaces," *Chemistry of Materials*, vol. 19, no. 21, pp. 5090–5101, 2007.

[58] S. M. O'Driscoll, C. T. O'Mahony, R. A. Farrell, T. G. Fitzgerald, J. D. Holmes, and M. A. Morris, "Toroid formation in polystyrene-block-poly(4-vinyl pyridine) diblock copolymers: combined substrate and solvent control," *Chemical Physics Letters*, vol. 476, no. 1–3, pp. 65–68, 2009.